

Senka Gudić^{1*}, Dario Kvirgić¹, Ladislav Vrsalović¹,
Mirko Gojić²

¹University of Split, Faculty of Chemistry and Technology, Split,
Croatia, ²University of Zagreb, Faculty of Metallurgy, Sisak, Croatia

Scientific paper

ISSN 0351-9465, E-ISSN 2466-2585

UDC:620.193.4

doi: 10.5937/ZasMat1802307G



Zastita Materijala 59 (2)
307 - 315 (2018)

Comparision of the corrosion behavior of AISI 304, AISI 316L and duplex steel in chloride solution

ABSTRACT

The corrosion behavior of stainless steels (AISI 304, AISI 316L and duplex steel) in NaCl solution was investigated using open circuit potential measurements, cyclic polarization and linear sweep voltammetry measurements. After cyclic polarization measurements electrode surfaces was investigated by light microscope.

Duplex steel have the most noble open circuit potential, the lowest corrosion current density and the largest width of the passive region indicates its highest corrosion resistance. Also, compared to other samples, duplex steel shows the possibility of self-healing of oxide film.

Increasing the concentration of Cl⁻ ion, the depassivation potential becomes more negative for all investigated samples. If the potential scan rate increases depassivation potential becomes more positive, meaning that a certain time (induction time) is needed for the pitting occurs after the actual depassivation potential is established. Depassivation potential and pitting corrosion nucleation time of investigated samples increase in order: AISI 304 < AISI 316L < duplex steel.

Light microscopy investigations of samples reveal pits on the surface of AISI 304 and AISI 316L steel while duplex steel surface is almost clear of any corrosion damage.

Keywords: corrosion, stainless steel, polarization, light microscopy.

1. INTRODUCTION

Stainless steels are important construction materials which are often used when high mechanical properties, weldability and good corrosion resistance are imperative [1-4].

Although stainless steels possess excellent resistance to general corrosion, they are susceptible to the localized corrosion attack such as pitting corrosion in chloride containing environment [5-7]. Corrosion resistance of stainless steels are related to the formation of an insoluble, relatively uncreative chromium oxide-hydroxide enriched passive surface film that forms naturally in the presence of oxygen (self-passivation), whose thickness is in the range from 1 to 10 nm [7-10]. Corrosion resistance of the passive film is determinate by the alloy composition and environmental conditions, to which stainless steels are exposed.

High content of Cr in the stainless steels leads to the formation of a complex spinel-type passive film (Fe,Ni)O(Fe,Cr)₂O₃ responsible for its high corrosion resistance [8,11,12]. Manganese has been traditionally considered as austenite former and is often added to increase nitrogen solubility [13]. Nevertheless, its addition is usually accompanied by reduction of pitting corrosion resistance, associated with the formation of manganese sulphide inclusions [14]. There is a certain correlation between resistance to pitting corrosion and the size of MnS inclusions: reducing the size of the inclusions leads to increase resistance to pitting corrosion [15]. Molybdenum is considered as one of the principal alloying elements in stainless steel which enhances the pitting corrosion resistance and expands the passive region of stainless steel [12,16].

The most corrosion damages of stainless steels occur in neutral to acidic solutions containing chloride ions. Chlorides are the most common cause of local destruction processes because they are strong acid anions, and many metal cations possess significant solubility in chloride solutions. In addition, chlorides are relatively small anions

*Corresponding author: Senka Gudić

E-mail: senka@ktf-split.hr

Paper received: 30. 04. 2018.

Paper accepted: 26. 05. 2018.

Paper is available on the website:

www.idk.org.rs/journal

with a high diffusion power which impedes passivation [17]. Pitting corrosion is considered to be an autocatalytic process - once when pit is formed and the corrosion process is initially localized in the pit area, there is a significant change in the medium within the pit which becomes impoverished by cathode reactants (eg. oxygen) and enriched with metal cations and chlorides. Inside the pit the pH value is reduced. The resulting chloride medium is very aggressive, prevents repassivation and encourages further growth of the pits [18].

The purpose of this study is to compare the corrosion behavior of duplex stainless steel with AISI 304 and AISI 316L stainless steels through electrochemical polarization studies in NaCl solution.

Table 1. Chemical composition of investigated stainless steels

Tablica 1. Kemijski sastav ispitivanih uzoraka nehrđajućeg čelika

Material	Chemical composition, wt.%
AISI 304	19.05% Cr, 10.00% Ni, 1.30% Mn, 0.52% Si, 0.04% C, 0.05% N, 0.02% S, 69.00% Fe
AISI 316L	16.64% Cr, 10.68% Ni, 2.53 % Mo, 0.47% Si, 0.002% C, 0.024% Nb, 0.009% S, 0.0045% P, 69.60% Fe
duplex steel	22.21% Cr, 5.47% Ni, 3.14% Mo, 1.52% Mn, 0.33% Si, 0.26% Cu, 0.012% C, 0.035% V, 0.012%, Nb, 67.00% Fe

Corrosion behavior of stainless steels was investigated with different electrochemical methods such as open circuit potential (E_{oc}), cyclic polarization and linear sweep voltammetry measurements in NaCl solutions at 20 °C. Electrochemical experiments were performed using a potentiostat PAR M273A. A three-electrode cell was used for measurements; the working electrode was test samples whereas the counter and the reference electrode was platinum sheet and saturated calomel electrode.

Just after immersing the tested electrode in the 0.5 mol dm⁻³ NaCl solution, the resulting open circuit potential was measured through the period of 45 min. After that, cyclic polarization measurements were performed in potential range of -0.2 V vs. E_{oc} to 0.6 V (i.e. to 1.2 V for duplex steel) with the scan rate of 0.1 mV s⁻¹.

Linear sweep voltammetry measurements were performed in different concentrations of NaCl solution (0.01, 0.05, 0.1, 0.5 and 1 mol dm⁻³) and with different scan rates (1, 5, 10, 50 and 100 mV s⁻¹).

After cyclic polarization measurements the surface of electrodes was investigated using light microscope MXFMS-BD, Ningbo Sunny Instruments co. with the magnification of 50 times.

2. EXPERIMENTAL

The chemical composition of the investigated samples was shown in Table 1.

The electrical contact for the electrochemical measurements was achieved by soldering the stainless steel samples with the copper wire and then isolated them with acrylic resin leaving only one side exposed to the test solution. Prior to each measurement the electrode surface (0.5 cm²) was ground successively with different grades of SiC paper down to 1200 grit. After that, the samples were ultrasonically cleaned in ethanol and deionized water and immersed in electrolyte solution.

3. RESULT AND DISCUSSION

Figure 1 presents the evolution of open circuit potential as a function of time for AISI 304, AISI 316L and duplex stainless steel in a 0.5 mol dm⁻³ NaCl solution. The open circuit potential (E_{oc}) reflect the composite results of the electrochemical reactions which take place at the electrode/solution interface. From the Figure 1 it is clearly visible that the most noble E_{oc} was observed for the duplex steel, while AISI 304 and AISI 316L exhibit similar E_{oc} values. Moreover, the values of E_{oc} for duplex steel and AISI 316L steel increases gradually towards a nobler direction during the immersion which indicate the formation and thickening of the protective passive film on their surfaces. The values of E_{oc} for AISI 304 steel slowly decrease with time which indicates the poorer protective properties of its oxide film compared to the AISI 316L and duplex steel.

The general corrosion behavior of AISI 304, AISI 316L and duplex stainless steel in 0.5 mol dm⁻³ NaCl solution was investigated by recording the cyclic polarization curves in wide potential range. The purpose of these measurements was to evaluate the possibility of passivation and repassivation of tested samples and determination of corrosion current density (i_{corr}) and corrosion potential (E_{corr}).

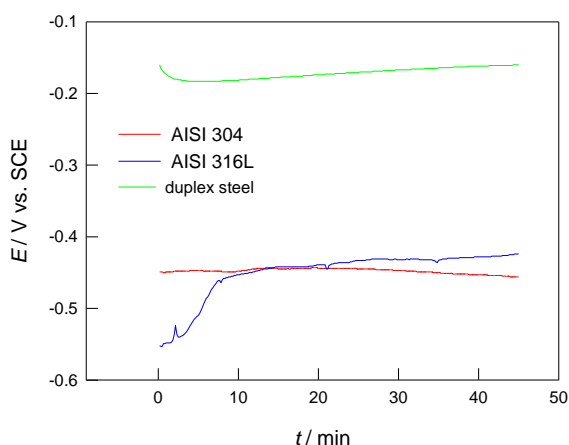


Figure 1. Evolution of open circuit potential as a function of time for investigated stainless steels in a $0.5 \text{ mol dm}^{-3} \text{ NaCl}$ solution

Slika 1. Vremenska promjena potencijala otvorenog strujnog kruga ispitivanih uzoraka nehrđajućeg čelika u $0.5 \text{ mol dm}^{-3} \text{ NaCl}$ otopini

Obtained results are presented on Figure 2 and Table 2. Significant differences in corrosion behavior of AISI 304 and AISI 316L compared with duplex steel can be noticed. Thus, negative hysteresis can be observed for duplex steel and positive hysteresis for AISI 304 and AISI 316L steels. Negative hysteresis occurs when reverse scan current density is less than for the forward scan and indicate that damaged passive film repairs itself and pits don't initiate.

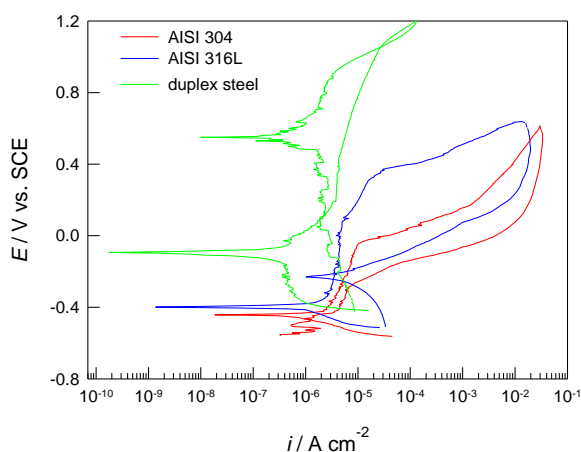


Figure 2. Cyclic polarization curves for investigated stainless steels in a $0.5 \text{ mol dm}^{-3} \text{ NaCl}$ solution

Slika 2. Cikličke polarizacijske krivulje ispitivanih uzoraka nehrđajućeg čelika u $0.5 \text{ mol dm}^{-3} \text{ NaCl}$ otopini

On the other hand, positive hysteresis occurs when reverse scan current density is greater than for forward scan and indicate that passive film is

damaged and not repaired and pits initiate on metal surface [19]. Comparing the anodic parts of the cyclic polarization curves it is apparent that the lowest values of anodic current density shows duplex steel and the highest AISI 304 steel. AISI 316L steel shows similar behavior as AISI 304 steel but with lower values of anodic current density.

As can be seen from Table 2 the lowest i_{corr} and the most positive E_{corr} have been obtained in measurements with duplex steel which also have the widest passive region which clearly indicates its highest corrosion resistance.

Table 2. Corrosion parameters of investigated stainless steels obtained from cyclic polarization measurements in $0.5 \text{ mol dm}^{-3} \text{ NaCl}$ solution

Tablica 2. Korozijski parametri ispitivanih uzoraka nehrđajućeg čelika dobiveni metodom cikličke polarizacije u $0.5 \text{ mol dm}^{-3} \text{ NaCl}$ otopini

	AISI 304	AISI 316L	duplex steel
$i_{\text{corr}} / \mu\text{A cm}^{-2}$	1.201	1.032	0.350
$E_{\text{corr}} / \text{V}$	-0.442	-0.399	-0.108

After cyclic corrosion measurement electrode surfaces were examined with light microscope with the magnification of 50 times, and the results of investigations have shown on Figure 3 (a-c). Pits are visible on the surface of AISI 304 and AISI 316L steel while duplex steel surface is almost clear of any corrosion damages.

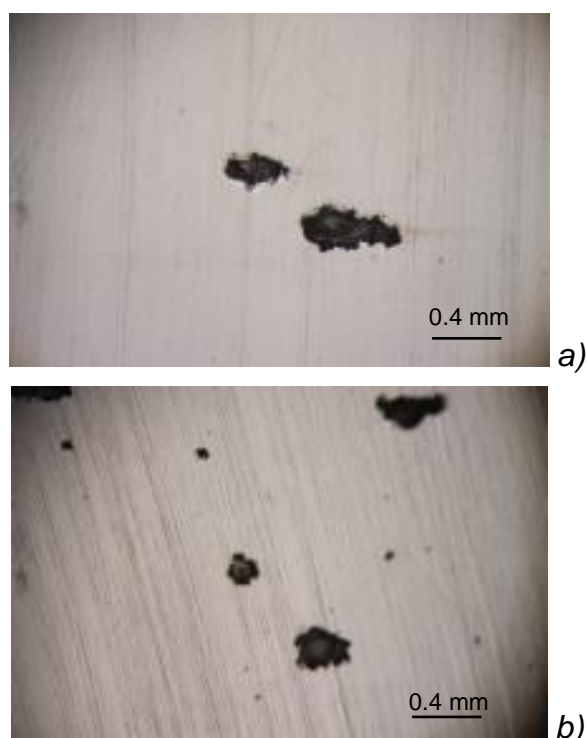




Figure 3. Light microscopy images of the electrode surfaces after cyclic polarization measurements for a) AISI 304, b) AISI 316L and c) duplex stainless steel

Slika 3. Mikroskopske snimke površina elektroda nakon mjerenja cikličkom polarizacijom za a) AISI 304, b) AISI 316L and c) duplex nehrđajući čelik

In this investigation special attention is dedicated to the depassivation of AISI 304, AISI 316L and duplex steel, therefore for each sample, polarization curves were recorded in different chloride ion concentrations (from 0.01 to 1 mol dm⁻³) with scan rate of 1 mVs⁻¹. Results of investigation for duplex stainless steel are shown in Figure 4.

By anodic polarization of duplex steel, after passing the passive potential range the depassivation potential (or potential of active anodic dissolution) is attained at which an abrupt increase in current takes place. Specifically, the oxide film at the metal surface is destroyed and local corrosion takes place with the creation of small pits on surface. If the potential is shifted further to the anodic direction, the current increases linearly.

According to the literature, the potential of pitting corrosion has several names: pitting potential, critical potential, breakdown potential and depassivation potential. On potential values that are more negative than depassivation potential pits do not appear, while on the more positive

potentials they are continually produced. At the exact pitting potential value, the created pits become deeper, without creation of new ones.

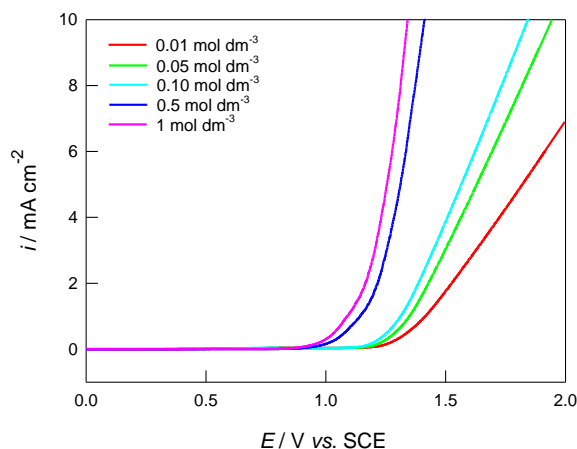


Figure 4. Anodic polarization curves for duplex stainless steel in a function of the concentration of NaCl

Slika 4. Anodne polarizacijske krivulje duplex nehrđajućeg čelika u funkciji koncentracije NaCl otopine ($v = 1 \text{ mV s}^{-1}$)

As can be seen from Figure 4 by increasing the concentration of chloride ions, depassivation potential (E_{dp}) for duplex steel becomes more negative. Furthermore, parallel with the displacement of E_{dp} towards the negative values, more steeper slopes of the linear part of the curve are observed, in the potentials range responsible for propagation of the pit, i.e., with potentials more positive than depassivation potential. The linear part of the curve (dE/di) defines the polarization resistance (R_p) of the corrosion process [20]. Many authors have explained this ohmic control by the presence of a thin, stable salt layer formed of an oversaturated solution present inside the pits, which gives some form of passivity [21]. Similar results were obtained for other investigated steel samples.

Table 3. Results of the analysis of anodic polarization curves for investigated stainless steels in a function of the concentration of NaCl solution ($v = 1 \text{ mV s}^{-1}$)

Tablica 3. Rezultati analize anodnih polarizacijskih krivulja za ispitivane uzorke nehrđajućeg čelika u funkciji koncentracije NaCl otopine ($v = 1 \text{ mV s}^{-1}$)

$c / \text{mol dm}^{-3}$	AISI 304		AISI 316L		duplex steel	
	E_{dp} / V	$R_p / \Omega \text{ cm}^2$	E_{dp} / V	$R_p / \Omega \text{ cm}^2$	E_{dp} / V	$R_p / \Omega \text{ cm}^2$
0.01	0.099	225.988	0.485	303.690	1.283	95.570
0.05	0.045	59.746	0.424	102.219	1.255	64.680
0.10	0.042	22.462	0.381	45.147	1.231	56.720
0.50	-0.044	5.875	0.359	12.20	1.184	20.220
1.00	-0.083	2.786	0.335	9.48	1.159	15.610

By analyzing the polarization curves E_{dp} and R_p was determined, and the obtained values in the function of chloride concentration for all examined samples are given in Table 3. Increasing the concentration of Cl^- ion, the E_{dp} becomes more negative for all investigated samples, while the R_p decreases considerably. Depassivation potential shift to the negative side greatly, which depends on the composition of the sample. Thus, the negative displacement potential of AISI 304 is ≈ 180 mV, for AISI 316L ≈ 150 mV and for duplex steel ≈ 120 mV.

Graphical representation of dependence of E_{dp} on $\log c$, can be described by the empirical equation:

$$E_{dp} = A + B \log c_{Cl^-} \quad (1)$$

The constants A and B can be determined from the section and slope of the linear part of $E_{dp} - \log c$ dependence (Figure 5) and the obtained values are given in Table 4. Values of the empirical parameters A and B for the investigated steel samples are very well matched with the data given in the literature, and this constant depends on the electrolyte temperature [22,23].

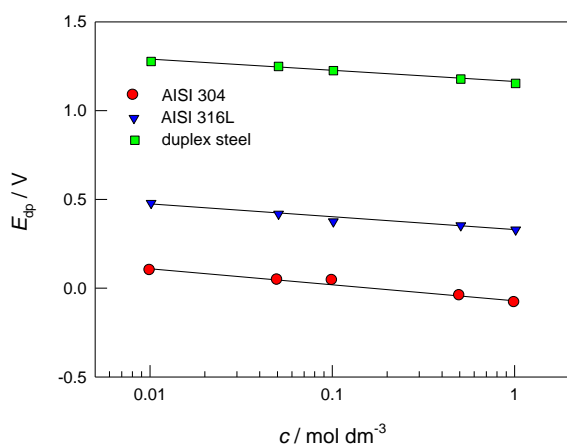


Figure 5. Dependence of depassivation potential on concentration of NaCl solution for investigated stainless steels ($v = 1 \text{ mV s}^{-1}$)

Slika 5. Ovisnost potencijala depasivacije ispitivanih uzoraka nehrđajućeg čelika o koncentraciji NaCl otopine ($v = 1 \text{ mV s}^{-1}$)

Table 5. Results of the analysis of anodic polarization curves for investigated stainless steels in 0.5 mol dm^{-3} NaCl solution in a function of potential scan rate

Tablica 5. Rezultati analize anodnih polarizacijskih krivulja za ispitivane uzorke nehrđajućeg čelika u 0.5 mol dm^{-3} NaCl otopini u funkciji brzine promjene potencijala

$v / \text{mV s}^{-1}$	AISI 304		AISI 316L		duplex steel	
	E_{dp} / V	$R_p / \Omega \text{ cm}^2$	E_{dp} / V	$R_p / \Omega \text{ cm}^2$	E_{dp} / V	$R_p / \Omega \text{ cm}^2$
1	-0.045	5.875	0.359	12.200	1.184	20.220
5	0.014	6.540	0.443	11.113	1.250	18.233
10	0.035	5.192	0.514	12.750	1.321	18.601
50	0.058	4.528	0.514	12.510	1.352	17.760
100	0.069	6.110	0.518	11.035	1.397	19.780

Table 4. Values of parameters A and B for investigated stainless steels in different concentration of NaCl solution ($v = 1 \text{ mV s}^{-1}$)

Tablica 4. Vrijednosti parametara A i B ispitivanih uzoraka nehrđajućeg čelika dobiveni u NaCl otopini različitih koncentracija ($v = 1 \text{ mV s}^{-1}$)

	A / V	$B / \text{V mol}^{-1} \text{ dm}^3$
AISI 304	-0.071	-0.090
AISI 316	0.330	-0.073
duplex steel	1.164	-0.063

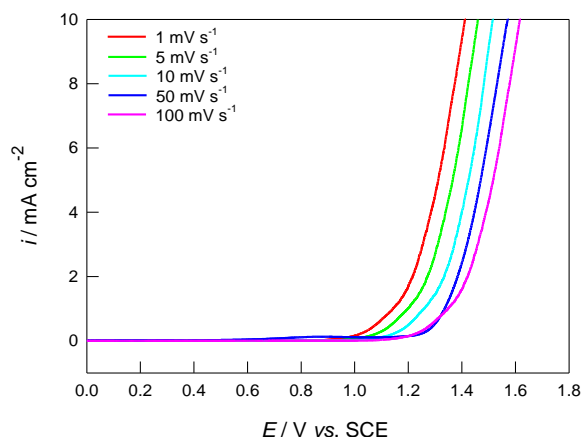


Figure 6. Anodic polarization curves for duplex stainless steel in 0.5 mol dm^{-3} NaCl solution in a function of the potential scan rate

Slika 6. Anodne polarizacijske krivulje duplex nehrđajućeg čelika u 0.5 mol dm^{-3} NaCl otopini u funkciji brzine promjene potencijala

Figure 6 and Table 5 show the influence of the potential scan rate on depassivation of stainless steel in 0.5 mol dm^{-3} NaCl. It can be noticed that the E_{dp} of all investigated samples becomes more positive if the potential change in the positive direction is achieved faster (this shift for AISI 304 is 110 mV, for AISI 316L 160 mV and for duplex steel 200 mV), which means that for evaluation of pitting it takes a certain amount of time (induction time) after the actual depassivation potential is established [21].

As shown in Table 5, irrespective of the E_{dp} shift towards more positive values, the rate of potential changes does not affect the value of polarization resistance. At all observed scan rates, similar values of R_p were obtained, whose value however depends on the composition of the examined sample and grows in order: AISI 304 < AISI 316L < duplex steel.

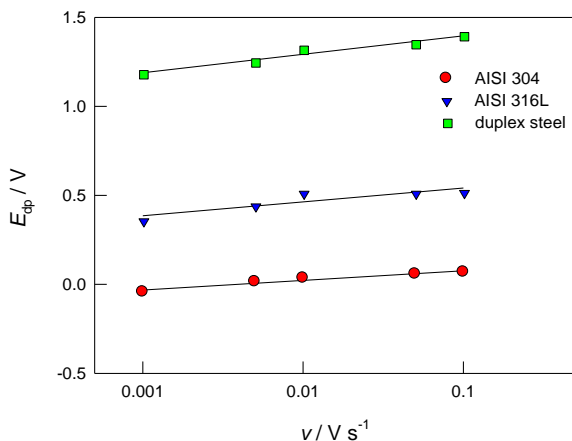


Figure 7. Dependence of depassivation potential on potential scan rate for investigated stainless steels in $0.5 \text{ mol dm}^{-3} \text{ NaCl}$ solution

Slika 7. Ovisnost potencijala depasivacije ispitivanih uzoraka nehrđajućeg čelika o brzini promjene potencijala u $0.5 \text{ mol dm}^{-3} \text{ NaCl}$ otopini

If we graphically depict the E_{dp} in a function of the $\log v$ (Figure 7), a linear dependence is obtained, which can be described by the relation:

$$E_{dp} = A + B \log v \quad (2)$$

A and B are constants and are listed in Table 6. Constant A is essentially the actual depassivation potential ($v = 0 \text{ mV s}^{-1}$), while B is the time needed for the induction of pitting corrosion. According to the literature numerical values of this constant depend on the electrolyte temperature [22,23].

Table 6. Values of parameters A and B for investigated stainless steels in $0.5 \text{ mol dm}^{-3} \text{ NaCl}$ solution in a function of potential scan rate

Tablica 6. Vrijednosti parametara A i B ispitivanih uzoraka nehrđajućeg čelika dobiveni u $0.5 \text{ mol dm}^{-3} \text{ NaCl}$ otopini kod različitih brzina promjene potencijala

	A / V	B / s
AISI 304	0.130	0.054
AISI 316L	0.619	0.078
duplex steel	1.500	0.104

The parameters A and B of the investigated samples increase in order: AISI 304 < AISI 316L < duplex steel. Namely, in the same order the depassivation potential becomes more positive, and the nucleation time of pitting corrosion increases. This behavior is the result of physical and chemical properties of the oxide films formed on the surface of tested samples.

Properties of the oxide films which form on the surface of stainless steels primarily depend on the chemical composition of the based metal, i.e. the content of the individual alloying elements in the investigated samples (Table 1). If the alloying element facilitates passivation of the steel, the properties of the oxide film will be better (higher resistance and thickness, more compact structure), which will ultimately increase the corrosion resistance of the metal in the aggressive media.

The role of alloying elements on metal passivation can be explained by the model proposed by Marcus [24]. The model is based on two fundamental properties of metals, such as:

- strength of the oxygen (or OH) chemisorption bond, δ_{M-O} , (reflected by the value of the heat of oxygen adsorption, $\Delta H_{ads(ox)}$) and
- the facility of conversion from the oxygen (or OH) monolayer to a 3D oxide in which a critical factor is disruption of the metal-metal bonds (reflected by metal-metal bond energy, δ_{M-M}) [24].

Passivation usually begins by adsorption of oxygen or OH from the water solution, followed by nucleation and oxide growth. Obviously, metals with high heat of oxygen adsorption are easily passivated. However, it is less apparent and less recognizable that the passive film formation requires additional activation energy for conversion of chemisorbed layer into 3D oxide, and that this process inevitably leads to a metal-metal interruption. Therefore the lower the energy required to disrupt metal-metal bonds, the lower the activation energy barrier for the conversion into 3D oxide [24]. The metals which adsorb oxygen (or OH) strongly and on which metal-metal bonds are easily broken will be very suitable for the passive oxide film growth. Hence, alloying elements with high energy adsorption of oxygen, and low metal-metal bonds energy, reinforce the passivation of the base metal. However, the easy metal-metal bond disruption will also accelerate metal dissolution. Therefore, fine balancing between the effect of metal-metal bonding energy and the effect of oxygen adsorption heat is crucial in design of alloys which can passivate.

Based on such considerations, it is possible to divide alloying elements on passivity promoters and dissolution moderators or blockers. In order to

make these ideas clearer, the diagram $\Delta H_{\text{ads(ox)}} - \varepsilon_{\text{M-M}}$ (Figure 8) is constructed on the basis of Marcus consideration [24].

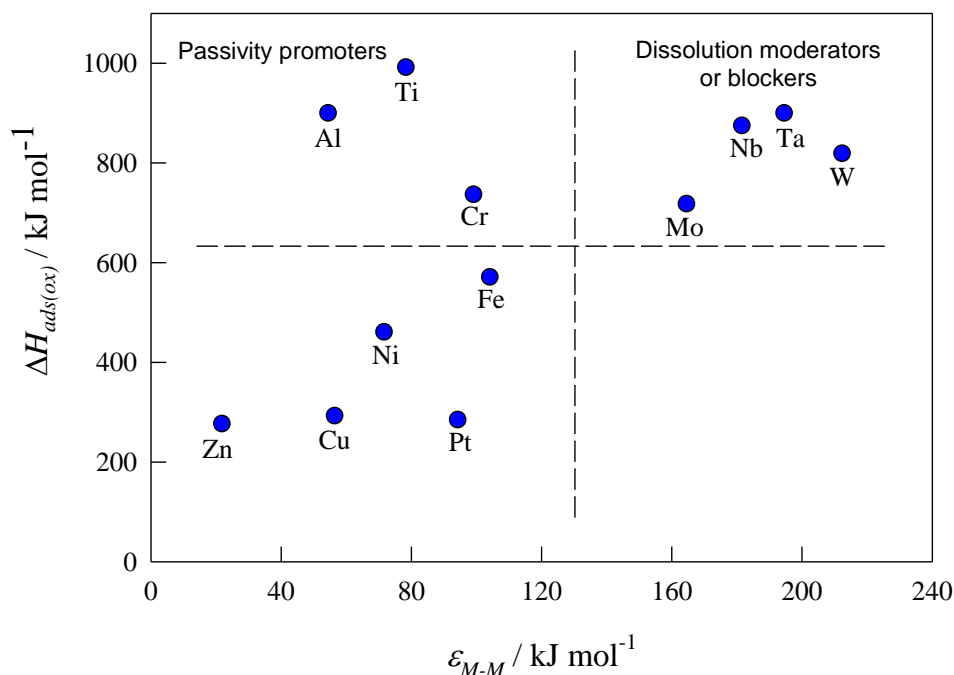


Figure 8. Passivity promoters and dissolution moderators according to the synergy between the $\Delta H_{\text{ads(ox)}}$ and $\varepsilon_{\text{M-M}}$ [24]

Slika 8. Legirajući elementi koji olakšavaju pasivaciju te elementi koji priječe otapanje metala na osnovu ovisnosti $\Delta H_{\text{ads(ox)}}$ o $\varepsilon_{\text{M-M}}$ [24]

Different metal groups can be seen on the diagram. In the upper left area of the diagram, are placed metals with high $\Delta H_{\text{ads(ox)}}$ and a relatively low $\varepsilon_{\text{M-M}}$: Cr, Al, Ti. This area of the diagram corresponds to passivity promoters, i.e. the alloying elements that facilitate passivation of the metal.

In the upper right-hand region of the diagram are metals with high $\varepsilon_{\text{M-M}}$ and high $\Delta H_{\text{ads(ox)}}$: Mo, Nb, Ta and W. The high value of $\varepsilon_{\text{M-M}}$ indicates the difficulty to break metal-metal bonds, so these elements can be dissolution moderators or blockers. Furthermore, the metals of this group also have a high amount of $\Delta H_{\text{ads(ox)}}$ so they do not lose the ability of passivation. They may participate in passivation and be incorporated in surface oxide film. Based on the ideas presented, it is interesting to compare the influence of key alloying elements such as Cr, Mo and Nb on the passivation of stainless steels, whose content in the tested samples mostly increases in order: AISI 304 < AISI 316L < duplex steel. The specific roles of Cr and Mo (or Nb) can be well understood in the framework of the proposed model. Namely, the behavior

of these elements in the initial stage of steel passivation is very different. Although the heat of oxygen adsorption on Cr, Mo and Nb is similar, the Cr-Cr bond energy is much lower than that of Mo-Mo and Nb-Nb [24]. A large amount of energy released during the adsorption of oxygen is able to easily disrupt Cr-Cr bonds, thus causing oxide nucleation much before completion of the adsorbed monolayer.

On the other hand, the Mo and Nb further improves the corrosion resistance of the stainless steels, especially in solution containing Cl^- in which pitting is a common occurrence. Namely, the high Mo-Mo and Nb-Nb bond strength causes a lowering of the dissolution rate by increasing the activation energy barrier for the disruption of metal-metal bonds on the surface [24]. This effect of alloying elements in the iron base ultimately results in the corrosion resistance of the tested samples growing in the same order, i.e. AISI 304 < AISI 316L < duplex steel. The content of the other elements in the individual samples also favors the increase of corrosion resistance according to sequence discussed.

4. CONCLUSIONS

In this paper, corrosion behavior of different types of stainless steels (AISI 304, AISI 316L and duplex steel) was studied in NaCl solution. From the analysis of the obtained results can be concluded as follows:

- Anodic polarization of all samples in NaCl solution results in the destruction of the natural oxide film and the occurrence of local activation of the surface with the creation of small pits. The damages of oxide film on duplex steel have tendency of self-healing.
- As the concentration of aggressive ions increases, the depassivation potential of all investigated stainless steel samples becomes more negative, while the polarization resistance of the corrosion process decreases considerably.
- If the change of potentials in the positive direction is realized faster, depassivation potential becomes more positive, meaning that a certain time (induction time) is needed for the pitting occurs after the actual depassivation potential is established.
- The potential scan rate does not affect the value of polarization resistance.
- Corrosion resistance of investigated stainless steels is following the order: AISI 304 < AISI 316L < duplex steel. Namely, the depassivation potential and pitting corrosion induction time of the examined samples increase in the same way.
- A key role in the corrosion resistance of the alloyed alloys has alloying elements such as Cr, Mo and Nb. Cr belongs to the elements which promote the passivation, while Mo and Nb in a group which prevents the dissolution of the metal.

5. REFERENCES

- [1] G.Gedge (2008) Structural uses of stainless steel – buildings and civil engineering, *Journal of Constructional Steel Research*, 64, 1194-1198.
- [2] S.K.Naha (2011) Stainless steel the green alloy, *Science Reporter* 48, 52-55.
- [3] S.Kožuh, M.Gojić, L.Vrsalović, B.Ivković (2013) Corrosion failure and microstructural analysis of AISI 316L stainless steel for ship pipeline before and after welding, *Kovove Materialy*, 51, 53-61.
- [4] S.Kožuh, L.Vrsalović, M.Gojić, S.Gudić, B.Kosec (2016) Comparison of the corrosion behavior and surface morphology of NiTi alloy and stainless steels in sodium chloride solution, *Journal of Mining and Metallurgy. Section: B, Metallurgy*, 52, 53-61.
- [5] B.Bobić, B.Jegdić (2005) Pitting korozija nehrđajućih čelika, deo I: teorijske osnove i metode ispitivanja, *Zaštita Materijala*, 46, 23-30.
- [6] B.Kulušić, Lj.Krstulović, J.Ivić (2004) Rupičasta koroziji čelika 304L u otopinama klorid-ionu u prirodnim slanim vodama, *Kemija u industriji*, 53, 1-5.
- [7] S.Kožuh, M.Gojić, M.Kraljić Roković (2008) The effect of PWHT on electrochemical behavior of AISI 316L weld metal, *Chem. Biochem. Eng. Q.*, 22, 421-431.
- [8] I.Juraga, V.Šimunović, Đ.Španiček (2007) Contribution to the study of effects of surface state of welded joints in stainless steel upon resistance towards pitting corrosion, *METABK*, 46, 185-189.
- [9] A.Pardo, M.C.Merino, M.Carboneras, A.E.Coy, R.Arrabal (2007) Pitting corrosion behavior of austenitic stainless steels with Cu and Sn additions, *Corros. Sci.*, 49, 510-525.
- [10] V.Alar, G.Barišić, B.Runje, Ž.Alar (2012) The influence of the surface finishing on the electrochemical behavior of austenitic and superaustenitic steels, *Mat.-wiss. U. Werkstofftech.*, 43, 725-732.
- [11] E.Jafari, M.J.Hadianfard (2009) Influence of surface treatment on the corrosion resistance of stainless steel in simulated human body environment, *J. Mater. Sci. Technol.*, 25, 611-614.
- [12] J.A.Platt, A.Guzman, A.Zuccari, D.W.Thomburg, B.F.Rhodes, Y.Oshida, B.K.Moore (1997) Corrosion behavior of 2205 duplex stainless steel, *Am J Orthod Dentofacial Orthop.*, 112, 69-79.
- [13] R.F.A. Jargelius-Pettersson (1998) Application of the pitting resistance equivalent concept to some highly alloyed austenitic stainless steels, *Corrosion*, 54, 162-168.
- [14] A.Pardo, M.C.Merino, A.E.Coy, F.Viejo, R.Arrabal, E.Matykina (2008) Pitting corrosion behavior of austenitic stainless steels – combining effects of Mn and Mo additions, *Corros. Sci.*, 50, 1796-1806.
- [15] B.V.Jegdić, B.M.Bobić, B.M.Radojković, B.Alić (2018) Formiranje i rast pitova na austenitnom nehrđajućem čeliku X5CrNi18-10 u prisustvu hlorida i sulfata, *Zaštita materijala*, 59(1), 92-99.
- [16] A.Pardo, M.C.Merino, A.E.Coy, F.Viejo, R.Arrabal, E.Matykina (2008) Effect of Mo and Mn additions on the corrosion behavior of AISI 304 and 316 stainless steel in H₂SO₄, *Corros. Sci.*, 50, 780-794.
- [17] I.Juraga, V.Šimunović, I.Stojanović (2007) Zavarivanje Cr-Ni čelika, korozijska postojanost, rukovanje, Seminar: Čelici otporni na koroziju (nehrđajući čelici), Pula, Hrvatska, 1-11.
- [18] I.Juraga, V.Šimunović, Đ.Španiček (2007) Contribution to the study of effects of surface state of welded joints in stainless steel upon resistance towards pitting corrosion, *METABK*, 46, 185-189.
- [19] W.S.Tait (1994) An introduction to electrochemical corrosion testing for practicing engineers and scientists, *Pair O Docks Publications*, St. Clair. Racine, Wisconsin, USA.
- [20] J.B.Bessone, D.R.Salinas, C.E.Mayer, M.Ebert, W.J.Lorenz (1992) An EIS study of aluminium barrier-type oxide films formed in different media, *Electrochim. Acta*, 37, 2283-2290.
- [21] T.R.Beck (1984) Salt film formation during corrosion of aluminum, *Electrochim. Acta*, 29, 485-491.

- [22] A.U.Malik, N.A.Siddiqi, S.Ahmad, I.N.Andijani (1995) The effect of dominant alloy additions on the corrosion behaviour of some conventional and high alloy stainless steels in seawater, *Corros. Sci.*, 37, 1521-1535.
- [23] A.U.Malik, P.C.Mayan Kutty, N.A.Siddiqi, I.N.Andijani, S.Ahmed (1992) The influence of pH and chloride concentration on the corrosion behaviour of AISI 316L steel in aqueous solutions, *Corros. Sci.*, 33, 1809-1827.
- [24] P.Marcus (1994) On some fundamental factors in the effect of alloying elements on passivation of alloys, *Corros. Sci.*, 36, 2155-2158.

IZVOD

USPOREDBA KOROZIJSKOG PONAŠANJA AISI 304, AISI 316L I DUPLEX ČELIKA U OTOPINI KLORIDA

Korozijско ponašanje različitih vrsta nehrđajućeg čelika (AISI 304, AISI 316L te duplex čelika) u NaCl otopini ispitano je mjerenjem potencijala otvorenog strujnog kruga te primjenom cikličke i linearne polarizacije. Nakon mjerenja cikličkom polarizacijom površine elektroda snimljene su svjetlosnim mikroskopom.

Duplex čelik pokazuje najpozitivniju vrijednost potencijala otvorenog strujnog kruga, najmanju gustoću korozijske struje i najšire područje pasivacije, što ukazuje na njegovu najveću korozijsku otpornost. Također, u usporedbi s drugim ispitivanim uzorcima, duplex čelik ima sposobnost obnavljanja površinskog oksidnog filma.

S porastom koncentracije kloridnih iona potencijal depasivacije svih ispitivanih uzoraka čelika postaje negativniji. Nadalje, ukoliko se promjena potencijala u pozitivnom smjeru ostvaruje brže, potencijal depasivacije postaje pozitivniji, što znači da je za pojavu pittinga potrebno izvjesno vrijeme (indukcijsko vrijeme) nakon što se uspostavi stvarni potencijal depasivacije. Potencijal depasivacije i vrijeme nukleacije pitting korozije ispitivanih uzoraka raste redom: AISI304 < AISI 316L < duplex čelik. Ispitivanjem uzoraka svjetlosnim mikroskopom uočena su oštećenja na površini AISI 304 i AISI 316L dok je površina duplex čelika gotovo neoštećena korozijom.

Ključne riječi: korozija, nehrđajući čelik, polarizacija, svjetlosna mikroskopija.

Naučni rad

Rad primljen: 30. 04. 2018.

Rad prihvaćen: 26. 05. 2018.

Rad je dostupan na sajtu: www.idk.org.rs/casopis